



## OPEN Implication of digestive functions and microbiota in the establishment of muscle glycogen differences between divergent lines for ultimate pH

Philippe Bochereau<sup>1</sup>, Sarah Maman Haddad<sup>2</sup>, Julien Pichon<sup>3</sup>, Christelle Rossignol<sup>3</sup>, Agnès Narcy<sup>1</sup>, Sonia Métayer-Coustard<sup>1</sup>, Cécile Berri<sup>1</sup>✉ & Elisabeth Le Bihan-Duval<sup>1</sup>✉

Both the quality of chicken meat and the quality of chicks are influenced by the level of breast muscle glycogen reserves. In order to study the role of digestive metabolism in establishing this muscular phenotype, we compared two divergent chicken lines for the ultimate pH (pHu) of the breast meat, a proxy for glycogen reserves. Males aged 4 weeks had twice the breast muscle glycogen content in the pHu- line (low pHu) than in the pHu+ line (high pHu). The increase in glycogen reserves (pHu-) was associated with a higher relative weight of the proventriculus and gizzard, as well as better apparent ileal digestibility of nitrogen and calcium. The diversity of the cecal microbiota was comparable, but three bacterial genera (*Lachnospira*, *Lachnospiraceae* UCG-010, *Caproiciproducens*) varied between the lines. The differences observed could lead to down-regulation of carbon fixation in prokaryotes and of the citrate cycle in the pHu+ line. RNA-seq analysis of the jejunum, the major site of nutrient absorption, revealed 149 genes differentially expressed (DE) between the lines, including several genes linked to immunity, hormonal response and circadian rhythms that are less expressed in pHu+ animals. Others involved in cell migration and proliferation, and more generally tissue morphogenesis, also differed between the lines. Among the DE genes, several co-localized with Quantitative Trait Loci (QTL) controlling pHu and selection signatures identified in the divergent lines, such as the gene coding for ghrelin, a hormone regulating appetite.

**Keywords** Chicken, Glycogen, Muscle, Gut, Microbiota, RNA-seq

Due to its low production costs, nutritional qualities and the absence of religious prohibitions, poultry meat has been increasingly consumed for several decades and has been the most commonly produced meat worldwide since 2017<sup>1</sup>. To meet this large market, the industry has implemented successful selection strategies and rearing practices to increase the growth rate and breast meat yield of broiler chickens. Unfortunately, these advances have been associated with a number of muscle disorders that affect meat quality. The first were associated with an abnormal rate or extent of postmortem pH drop, resulting in acidic or pale, soft, exudative meat (referred to as PSE-like meat) or dark, firm, dry meat (referred to as DFD-like meat). More recently, structural defects, such as white striping (WS), wooden breast (WB), and spaghetti meat (SM), which affect the technological, sensory and nutritional properties of meat, have been identified<sup>2–5</sup>. In chickens, the ultimate pH (pHu) of the meat is a key quality determinant and is mainly influenced by the amount of glycogen present in the muscle at the time of slaughter. The higher the glycogen content is, the more acidic, pale and exudative the meat is. The amount of glycogen stored in the breast muscle, which can be estimated from the glycolytic potential at slaughter, is highly heritable (h<sup>2</sup> between 0.3 and 0.5)<sup>6</sup> and genetically negatively correlated with the ultimate pH (rg = -0.97)<sup>7</sup>.

Because of the importance of this physiological parameter, two broiler lines, namely, pHu- (i.e., low pHu) and pHu+ (i.e., high pHu), were selected divergently from a fast-growing chicken line according to the breeding value for breast meat pHu measured at 6 weeks of age<sup>8</sup>. These two lines provide an original model for studying

<sup>1</sup>BOA, INRAE, Université de Tours, 37380 Nouzilly, France. <sup>2</sup>SIGENAE, INRAE, ENVT, GenPhyse, Université de Toulouse, 31326 Castanet Tolosan, France. <sup>3</sup>ISP, INRAE, Université de Tours, 37380 Nouzilly, France. ✉email: cecile.berri@inrae.fr; elisabeth.duval@inrae.fr

the genetic and physiological mechanisms underlying the variations in the ultimate pH and muscle glycogen content of meat in chickens, as well as the related meat quality parameters. At six weeks of age, during the selection period, the pHu – chickens had more glycogen in their pectoral muscles than did the pHu + chickens<sup>9</sup>. The various studies carried out on the two divergent lines showed that increasing the pHu of breast meat by selection changed the pHu of the thigh meat in the same direction. This resulted in improvements in many breast quality criteria, such as reduced drip loss and increased processing yield and tenderness after cooking. However, a higher pHu was also associated with an increased frequency of white striping defects in the pHu + line<sup>10</sup>. This could be partly explained by the higher breast meat yield in this line but also by more intense muscle fibre degeneration and regeneration processes<sup>8</sup>. Differences in muscle glycogen are present from hatching onwards and are also associated with variations in chick quality<sup>11,12</sup>. These disparities reflect a profound change in the energy metabolism of growing animals, as well as that of breeding females, whose laying performance and internal and external egg quality levels are affected by selection<sup>13,14</sup>. More generally, the two lines show differences in energy production pathways, mainly based on carbohydrate metabolism in the pHu- line or involving the activation of alternative pathways such as amino acid catabolism and fatty acid oxidation in the muscle of the pHu + line<sup>15,16</sup>. These metabolic changes could contribute to the lower feed efficiency of the pHu + broilers<sup>17</sup>.

Genomic analysis of the divergent lines revealed several selection signatures and quantitative trait loci (QTLs) for the ultimate pH of breast or thigh meat that encode genes involved in human glycogen storage diseases (GSDs) whose abundance or functionality could strongly modulate the levels of glycogen stores<sup>18</sup>. Several studies, particularly those conducted in humans and mice, have also suggested a role for the gut microbiota in determining muscle glycogen reserves<sup>19</sup>. In mice, suppression of the intestinal microbial flora induces significant reductions in glycogen reserves and muscle capacity, phenomena that are reversible by natural reintroduction of the microbiota<sup>19</sup>. In chickens, and more specifically in the divergent pHu lines, the role of digestive function in the determination of glycogen reserves has not been studied.

The microbial ecology and metabolic activities of the digestive system have long been recognized as factors contributing to broiler performance. The gut microbiota is known to play essential roles in chicken digestion, nutrient absorption, sugar breakdown and essential vitamin production, and the composition of the microbiota has been shown to be associated with parameters such as growth rate and feed efficiency<sup>20–22</sup>. In addition, imbalances in the diversity, abundance and composition of microorganisms can lead to dysbiosis and the subsequent development of irritable bowel syndrome<sup>23</sup>. More generally, the availability of nutrients to tissues can be modulated by the ability of the digestive tract to absorb nutrients, depending on its morphology and metabolic properties. The aim of this study was to investigate the role of digestive function, in determining glycogen stores in chicken muscle, a key determinant of muscle functionality and meat quality. To this end, we compared the morphological, histological, microbial and molecular profiles of the digestive tracts between two divergent lines for the ultimate pH of breast meat, a proxy for muscle glycogen stores.

## Results

### Phenotypic characterization of the divergent lines

A difference of more than two was detected between the two lines for the glycolytic potential (GP) of the breast muscle, with a mean value of 229.8  $\mu\text{mol/g}$  in the pHu- line compared with 100.7  $\mu\text{mol/g}$  in the pHu + line ( $p = 4.23\text{E}-12$ ).

As shown in Additional Table 1, body weight at 4 weeks was 5.7% greater in the pHu- line than in the pHu + line.

Regarding the morphology of the digestive tract, individuals from both lines had similar relative weights of the duodenum, jejunum, ileum and caecum (Additional Table 1). In contrast, a 28.7% greater relative weight

ENSEMBL gene ID	Symbol	Chromosome	Start–end (bp)	Marker position (bp)	Marker Name	Trait
ENSGALG00010004934	KIAA1524	1	87,776,519–87,809,749	88,797,285	GGaluga031114	SART-pHu
ENSGALG00010013778	Novel gene	1	108,994,729–108,995,869	109,580,018	Gga_rs13920866	SART-pHu
ENSGALG00010009123	EMILIN1	3	104,303,618–104,309,725	105,066,175	Gga_rs14408993	SART-pHu
ENSGALG00010009227	ATRAID	3	104,323,632–104,328,461	105,066,175	Gga_rs14408993	SART-pHu
ENSGALG00010019047	GHRL	12	19,630,806–19,633,370	19,288,984	Gga_rs14049172	PM-pHu
ENSGALG00010019065	CAND2	12	19,641,317–19,657,048	19,288,984	Gga_rs14049172	PM-pHu
ENSGALG00010022455	C7orf50	14	2,281,425–2,378,309	3,272,632	Gga_rs14071447	PM-pHu
ENSGALG00010003731	LOC121106934	16	1,327,869–1,330,885	2,217,697	Gga_rs15026791	PM-pHu
ENSGALG00010002333	MHCYL	16	1,549,214–1,552,109	2,217,697	Gga_rs15026791	PM-pHu
ENSGALG00010002595	Novel gene	16	2,056,012–2,056,700	2,217,697	Gga_rs15026791	PM-pHu
ENSGALG00010002955	BLEC1	16	2,174,268–2,185,542	2,217,697	Gga_rs15026791	PM-pHu
ENSGALG00010002991	BLB1	16	2,184,974–2,187,386	2,217,697	Gga_rs15026791	PM-pHu
ENSGALG00010003022	BLB2	16	2,192,779–2,194,325	2,217,697	Gga_rs15026791	PM-pHu

**Table 1.** List of genes differentially expressed in the jejunum of the pHu + and pHu- lines that colocalize with QTL regions controlling ultimate pH in chicken Pectoralis major (PM-pHu) or Sartorius (SART-pHu) muscles. QTL region was defined as the 2 Mb region surrounding the most significant marker detected in GWAS analysis.

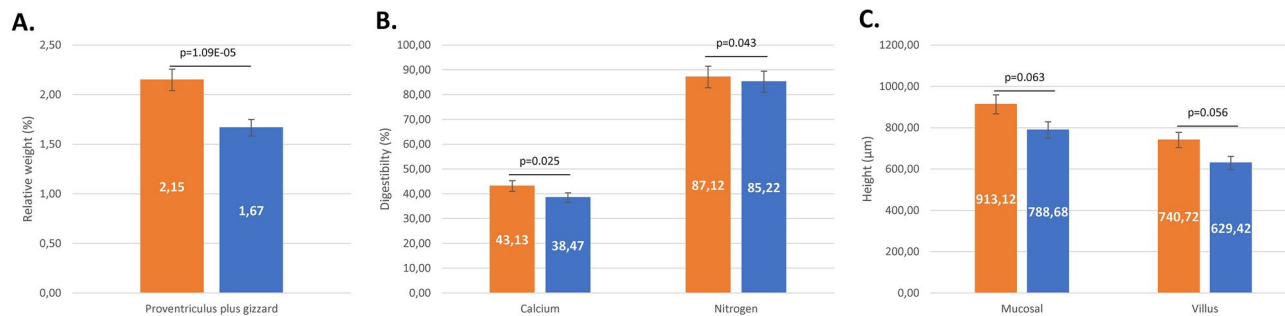


**Fig. 1.** Differences in morphological (A), digestibility (B) and histological (C) parameters between pHu- and pHu+ lines (N = 15 per line). In orange the pHu—line and in blue the pHu+ line.

ENSEMBL gene ID	Symbol	Chromosome	Gene position (in pb)	Marker-start	Marker-end	Generations*
ENSGALG00010006004	DCLRE1C	1	8,046,903–8,059,742	Gga_rs13826175	Gga_rs14792165	1/2/3/4/5
ENSGALG00010001222	ZNF800	1	21,002,064–21,064,015	Gga_rs13834995	GGaluGA010403	1/2/3/4/5
ENSGALG00010014241	Novel gene	1	32,737,556–32,740,706	Gga_rs15226289	GGaluGA011179	3
ENSGALG00010002033	Novel gene	2	91,465,114–91,469,533	Gga_rs14219779	GGaluGA158657	5
ENSGALG00010020340	DCAF5	5	27,643,840–27,711,265	Gga_rs14526966	Gga_rs16483831	1
ENSGALG00010023869	DOCK7	8	27,186,874–27,274,379	Gga_rs14656403	GGaluGA333330	4/5
ENSGALG00010027044	Novel gene	8	27,275,046–27,281,840	Gga_rs14656403	GGaluGA333330	4/5
ENSGALG00010023249	IL12RB2	8	28,334,716–28,351,018	Gga_rs14656403	GGaluGA333330	4/5
ENSGALG00010010056	Novel gene	11	16,497,586–16,500,093	Gga_rs14027883	Gga_rs14028221	2/3/4
ENSGALG00010019047	GHRL	12	19,630,806–19,633,370	Gga_rs15675057	Gga_rs15675542	1/2
ENSGALG00010019065	CAND2	12	19,641,317–19,657,048	Gga_rs15675057	Gga_rs15675542	1/2
ENSGALG00010000562	Novel gene	15	11,922,199–12,162,548	Gga_rs15786648	Gga_rs15787069	1

**Table 2.** List of genes differentially expressed in the jejunum of the pHu+ and pHu- lines that colocalize with selection signatures determined after five generations of selection<sup>18</sup>. \*Generation at which regions under selection were detected.

of the proventriculus plus gizzard was found in the pHu- line than in the pHu+ line (Fig. 1A). In terms of ileal digestibility, the pHu- line showed greater digestibility of calcium and nitrogen, unlike the digestibility of phosphorus, which did not differ between the two lines (Fig. 1B). Markers of digestive health (i.e., alkaline phosphatase activity, haptoglobin and total antioxidant capacity) did not differ between the two lines at the jejunal level (Additional Table 1). Histological characterization of the jejunum did not reveal any significant differences in crypt depth, villus width, or submucosal or muscularis thickness (Additional Table 1). However, the pHu- line tended to have greater mucosal thickness (913 µm versus 789 µm,  $p=0.063$ ) and greater villus height (741 µm versus 629 µm,  $p=0.056$ ) than did the pHu+ line (Fig. 1C).

### Jejunum transcriptomic profiles of the two lines

We obtained between 63 and 121 million sequences per sample by RNA sequencing. To align these sequences with the GalGal7 reference genome in the Ensembl database, we used the STAR tool. STAR succeeded in aligning the sequences with rates between 81 and 89%, indicating excellent alignments. Among the aligned sequences, we identified an average of 50 million unique sequences among the different samples. All the aligned sequences had excellent FastQC quality, with a minimum of 33.8. This measure assesses the quality of high-throughput sequence data, considering that the optimal measure of sequence quality lies between 28 and 34. In total, we identified 29,859 genes, 24,134 of which (i.e., 80.8%) exhibited detectable expression in the jejunum. Using the DESeq2 package, we performed biostatistical analyses, which revealed that 149 genes were differentially expressed (DE) between the two lines. Among these 149 genes, 91 were overexpressed in the pHu- line, while 58 genes were overexpressed in the pHu+ line (Additional Table 2). Of the 149 DE genes, 76 (51%) were identified by a known gene name, while the remaining 73 were classified as novel genes.

To better understand the biological functions related to the DE genes, we performed a functional analysis based on Gene Ontology (GO) analysis. All expressed genes, whether differentially expressed or not, were annotated by GO for biological process. Of the 29,859 expressed genes, 12,511 had at least one functional GO term in the Ensembl database (41.9%). An enrichment test was performed on the lists of genes overexpressed in the pHu+ and pHu- lines, using all expressed genes as a background for the analysis. Of our 76 identified DE genes, only 26 were associated with significantly enriched GO terms ( $p < 0.001$ ). Among the 42 identified enriched GO terms, 26 were mainly associated with genes overexpressed in the pHu- line, while 3 were mainly

associated with genes overexpressed in the pHu + line (Fig. 2 and Additional Table 3). The remaining 13 enriched GO terms were associated with genes from both the pHu- and pHu + lines in equal proportions (Fig. 2).

Among the 26 enriched GO terms related to genes overexpressed in the pHu- line (Fig. 2 and Additional Table 3), 8 (GO:0016477, GO:0061383, GO:0003344, GO:0060039, GO:0001937, GO:0050680, GO:1901890, and GO:0099072) were related to morphogenesis and tissue development (including biological regulation and anatomical development of tissue structure); 8 (GO:0032355, GO:0071392, GO:0043627, GO:0044344, GO:0071774, GO:0002792, GO:0046676, and GO:0090278) were related to stimulus response; 7 (GO:0045321, GO:0046649, GO:0002694, GO:0051249, GO:0050867, GO:0002696, and GO:0051251) were related to immunity-related processes; and 2 (GO:0007622 and GO:0048512) were related to rhythmic and circadian behaviour. Regarding the enriched GO terms related to genes overexpressed in the pHu + line, we identified 3 GO terms related to morphogenesis and tissue development and, more specifically, to microtubule organization (GO:0061842) and centrosome localization (GO:0051642 and GO:0051660). Of the 13 enriched GO terms shared between the pHu- and pHu + lines (Fig. 2), 10 (GO:0002396, GO:0002399, GO:0002501, GO:0002503, GO:0048002, GO:0002495, GO:0002504, GO:0019884, GO:0002478, and GO:0019886) were involved in immunity-related processes (in particular, the major histocompatibility complex (MHC) type II complex and antigen presentation), and 3 (GO:0072528, GO:0009112, and GO:0046112) were related to the metabolic processes of organo-nitrogen compounds.

To determine whether some of the DE genes found in the jejunum colocalized with genomic regions of interest, they were repositioned with respect to the pHu QTLs in breast and thigh meat as well as the selection signatures previously identified in the divergent lines<sup>18</sup>. QTL intervals were defined as regions of 1 megabase before and after the most significant genetic marker. A total of 13 DE genes were located in QTLs controlling *sartorius* (thigh) ultimate pH (4 genes) or *pectoralis major* (PM) ultimate pH (9 genes) (Table 1). We also identified 12 DE genes belonging to regions under selection (Table 2). The chromosome 12 region identified in generations 1 and 2 contained the GHRL and CAND2 genes, which also colocalized with a QTL controlling the ultimate pH of breast meat.

### Exploring the diversity, composition, and functions of the caecal microbiota of the pHu lines.

Sequencing of 30 caecal content samples (15 each line) yielded a total of 955,639 high-quality sequences from the Illumina MiSeq platform. The number of sequences per sample ranged from 20,133 to 38,351. At the end of the matching process, we were able to match all 955,639 sequences. After applying various filtering steps, such as removing sequences containing ambiguous base pairs, long contigs, nonspecific sequences and chimeric sequences, we obtained 511,449 unique sequences. Of the eliminated sequences, 289,467 could not be matched or were not the correct size, while 154,723 were identified as chimeric sequences. The remaining 511,449 high-quality sequences were divided into 25,487 different operational taxonomic units (OTUs). Using different filters based on abundance, coverage and identity, we eliminated 24,833 OTUs, corresponding to 36,853 sequences. As a result, caecal microbiota analysis was performed on 654 OTUs representing 474,596 sequences.

The above results were integrated into Shiny Migale for an in-depth analysis of the caecal microbiota. First, we calculated the alpha and beta diversity indices of the caecal bacterial communities of each line, pHu + and pHu-. To compare all samples under equivalent conditions, rarefaction with a sequencing depth of 13,000 reads was performed.

We identified 654 OTUs originating from 4 phyla, 5 classes, 17 orders, 33 families, and 83 genera. The massively dominant phylum was Firmicutes (with an average abundance of 93.9%), primarily consisting of

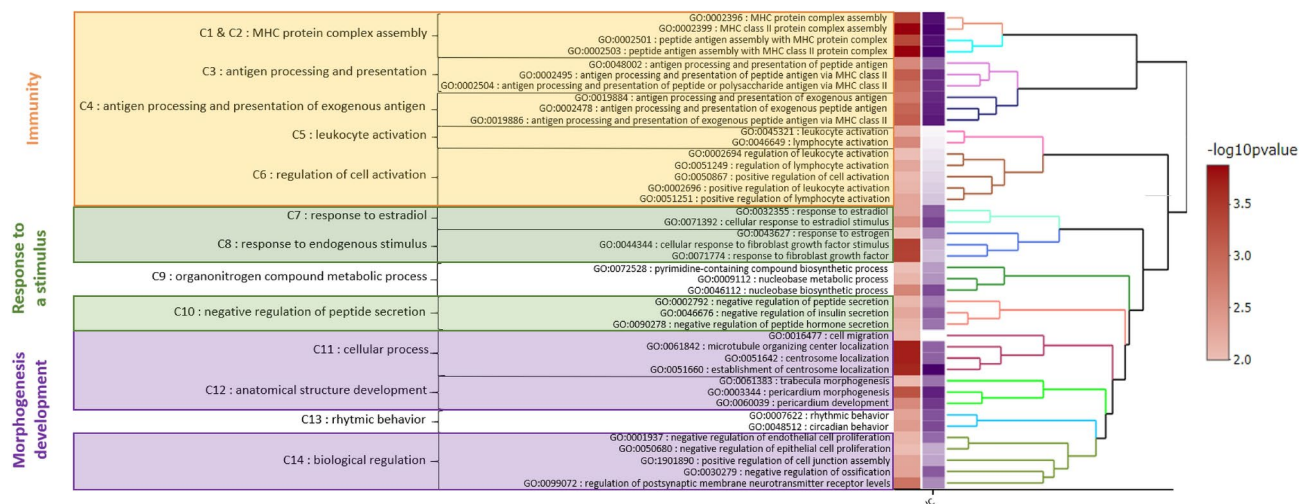


**Fig. 2.** Hierarchical clustering of enriched GO terms obtained from the set of DE genes in jejunum. The clustering heatmap plot obtained by VISEAGO combines the dendrogram of enriched GO terms based on semantic similarity, the heatmap of  $-\log_{10}(P\text{-value})$  from the functional enrichment test and the information content (IC) of the GO terms (with a colour scale from white for 0 to dark purple for 10).

Clostridia (91.9%) and Bacilli (8.1%). Firmicutes was followed by the less abundant Bacteroidetes (average abundance of 3.61%), Proteobacteria (average abundance of 2.42%), and Actinobacteria (average abundance of 0.07%). Regardless of the methodology used, Shannon diversity or the inverse Simpson diversity (InvSimpson) index, no differences in alpha diversity (i.e., species richness) were detected between the two lines. Regardless of the calculation method used (Bray–Curtis, Jaccard or UniFrac similarity indices), the beta diversity (i.e., species composition) was also similar between lines.

No differences in abundance were observed at the level of higher bacterial classifications, such as phylum, class or order. However, at the level of bacterial families, and genera, we found significant differences in abundance between the two lines for three genera, collectively representing less than 1% of the total caecal microbiota (Fig. 3.A). *Lachnospira* was identified by one OTU, and *Lachnospiraceae UCG-010* was identified by two OTUs; both showed greater relative abundances in the pHu- line, with P values of 0.0169 and 0.0301, respectively, while *Caproiciproducens*, identified by one OTU, was found in greater abundance ( $p=0.0115$ ) in the pHu+ line (Fig. 3B). The abundances of six other genera, representing less than 1% of the caecal microbiota, tended to differ ( $p < 0.1$ ) between the two lines (Additional Table 4).

In silico enrichment analysis of the average profiles of the microbiota of each line revealed 118 different metabolic pathways grouped into 6 major functions (Fig. 3C). On average, the metabolic pathways identified were grouped as follows: metabolism (75.2%), genetic information processing (15.8%), cellular processes (5.4%), environmental information processing (2.9%), organismal systems (0.5%), and human diseases (0.19%). The general profile of the caecal microbiota did not differ between the pHu+ and pHu- lines. However, two metabolic pathways were significantly affected by divergent selection: carbon fixation in prokaryotes (ko00720), which was overrepresented in the pHu- line (1.081% vs. 1.070%,  $p=0.05$ ), and the citrate cycle (ko00020), which was overrepresented in the pHu+ line (0.901% vs. 0.88%,  $p=0.035$ ).

## Discussion

In chickens, muscle glycogen reserves have a major impact on meat quality not only by influencing its ultimate pH but also by affecting other metabolic and cellular processes that may be involved in the occurrence of defects affecting the integrity of muscle tissue<sup>16</sup>. The muscle glycogen reserves may also affect other physiological functions, particularly those related to egg production or early chick development<sup>11,13</sup>. Recent studies in mice have shown that disturbances in the gut microbiota can affect muscle glycogen reserves, with consequences for contractile activity and fatigability<sup>19</sup>. Little is known about the links between digestive and muscular functions in chickens. This study aimed to identify the extent of changes at the digestive level, including microbiota

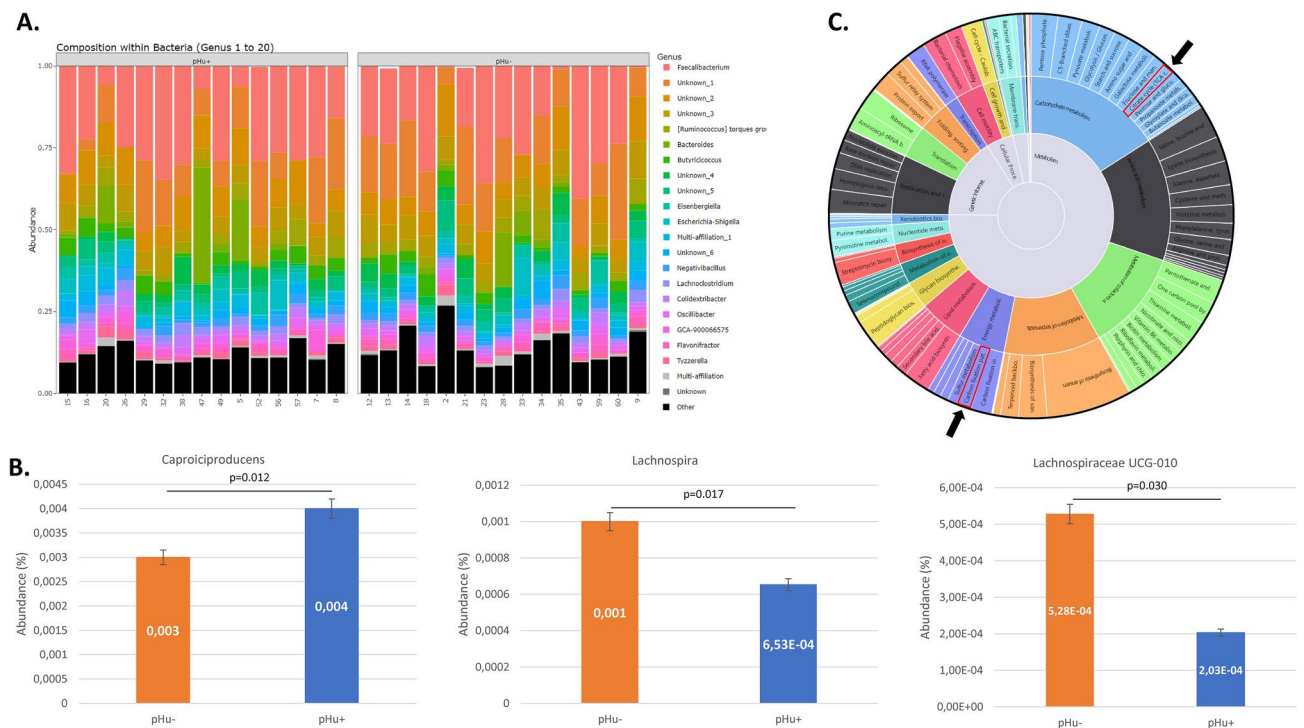


**Fig. 3.** Composition of the caecal microbial community in pHu- and pHu+ lines. Stacked bar graphs showing the relative abundances of the different bacterial genera in all samples from the pHu- and pHu+ lines (A). Diagram of the three significant bacterial genera between pHu- and pHu+ lines. In orange, the pHu- line and in blue, the pHu+ line (B). Hierarchical classification of pathways based on subgroup identification and pathway names, starting from the inner ring outwards (C). The two black arrows indicate the two metabolic pathways that were differentially abundant between the pHu+ and pHu- lines (surrounded in red).

composition, that could be linked to variations in muscle energy reserves, using original divergent lines for the ultimate pH of breast meat, a proxy for glycogen content.

In the 15th generation of selection, the difference in muscle glycogen between lines was much greater (2.3× in the pHu- line compared to pHu+) than that observed in the 6th generation (1.3×), although in that case, the measurement was made 5 days after hatching<sup>11</sup> or at slaughter age (6 weeks)<sup>15</sup> instead of at 4 weeks. We observed that the reduced muscle glycogen content in the pHu+ line was associated with a lower relative development of the proventriculus and gizzard and a tendency towards weaker growth. In chickens, divergent selection for digestive efficiency measured at 3 weeks of age in broilers has shown that good digesters have a greater relative weight of the proventriculus and gizzard than poor digesters<sup>24</sup>. Interestingly, in the 14th generation of selection, owing to the individual monitoring of feed intake, chickens of the pHu- line had a feed efficiency 5% greater than that of chickens of the pHu+ line from Day 12<sup>17</sup>. The greater development of the upper part of the gastrointestinal tract in the pHu- line probably favours enzymatic, chemical and mechanical digestion by increasing the secretion of hydrochloric acid and pepsinogen production in the proventriculus as well as the grinding of the digesta in the gizzard<sup>25</sup>. Rather logically, we observed higher digestibility coefficients for nitrogen in the pHu- line<sup>26</sup>. The difference in digestibility between calcium and nitrogen, but not phosphorus, can also be explained by the dietary absence of microbial phytase, an enzyme that plays a crucial role in the breakdown of phytate phosphorus. In addition, phosphorus is present in different forms in the diet, and these forms can be degraded and absorbed at different rates. Thus, the combination of these factors may explain why we observed differences in digestibility for calcium and nitrogen but not necessarily for phosphorus. The greater villus height observed in the jejunum in the pHu- line could also play a role in improving nutrient digestibility, as a greater amount of villus surface is likely to increase the surface area available for nutrient absorption in this part of the small intestine, where proteins, lipids, carbohydrates and calcium-, iron- and fat-soluble vitamins are absorbed<sup>22,27</sup>.

The digestive system serves several important functions. First and foremost, it is responsible for digesting feed, absorbing nutrients and eliminating waste. In addition, the gastrointestinal tract plays a crucial role in health, acting as a protective barrier against pathogens. The immune system must actively prevent these agents from entering the blood and lymph, largely due to the low pH of the stomach and the presence of mucus containing IgA antibodies that neutralize microorganisms. In addition, good intestinal bacteria play vital roles in various body functions, such as fermenting unused energy substrates, boosting the immune system, preventing the proliferation of pathogenic bacteria and producing vitamins<sup>25</sup>.

The present study revealed that selection of breast muscle pHu affects the expression of 149 genes in the jejunum. This number of DE genes, which was approximately 10 times lower than that found in the breast muscle at the 6th generation of selection<sup>16</sup>, was consistent with the expectation of more direct effects in the tissue targeted by selection and more indirect effects in the jejunum. Our previous study demonstrated that selection of pHu in breast meat primarily affected the transcription of many genes involved in carbohydrate and energy metabolism, which were upregulated in the pectoral muscle of the pHu- line, while many other genes involved in protein degradation, muscle remodelling and the response to oxidative stress were upregulated in the pHu+ line<sup>16</sup>. Here, we show that at the jejunal level, transcriptional regulation induced by selection affected several genes linked to immunity and hormonal response, which are generally less highly expressed in pHu+ animals, and several other genes involved in migration and cell proliferation and, more generally, in tissue morphogenesis, which also differed between lines.

Among the genes differentially expressed and/or located in QTLs controlling chicken meat pHu or in selection signatures, several are of particular interest because of their pleiotropic effects on various essential gut functions, potentially influencing cell turnover, immunity and digestion. This is the case for the GHRL gene, whose expression was upregulated more than twofold in the pHu- line. The GHRL gene encodes the prepropeptide of ghrelin/obestatin, which is known to stimulate appetite in mammals<sup>28</sup> but to induce satiety in chickens<sup>29</sup>. In this species, ghrelin is involved in the regulation of appetite, energy homeostasis and pituitary, gastrointestinal, cardiovascular and immune system functions. In addition, GHRL promotes lipolysis, regulates energy homeostasis by interacting with glucocorticoids and insulin, and contributes to anti-inflammatory activities, as well as to autocrine, paracrine and endocrine communication. Ghrelin directly influences the contractile activity of smooth muscle cells, particularly in the upper intestine, such as the proventriculus, thereby promoting nutrient availability in the gut<sup>30</sup>. Data obtained in rats in a model of intestinal damage due to irradiation have also shown the beneficial effects of ghrelin administration on limiting intestinal apoptosis and preserving the morphology of villi and crypts as well as the protective role of the intestinal epithelial barrier<sup>31</sup>.

We also identified a locus of 20 kb on chromosome 16 that controls breast meat pHu and contains three genes, BLEC1, BLB1 and BLB2, that were differentially expressed between pHu lines and are involved in the immune response. The BLEC1 gene encodes a natural killer receptor that binds MHC class I molecules. This interaction between the BLEC1 receptor and MHC molecules is particularly important for the recognition of infected or tumour cells by the immune system<sup>32</sup>. The BLB1 and BLB2 genes encode MHC type II proteins, which play essential roles in the immune system by enhancing antigen presentation to T lymphocytes<sup>33</sup>. It has been shown in several Galliformes species, including chickens, that only BLB2 is highly expressed and is considered dominant in the intestine<sup>33</sup>. However, the same study also reported the possibility of genetic exchanges between BLB1 and BLB2 in certain populations of pheasants and domestic chickens, suggesting concerted evolution. This could explain why, in a more recent study, BLB2 appeared to be expressed in a wide variety of tissues and cell lines, while BLB1 was poorly expressed except in the intestine, suggesting a general BLB2 system in many tissues and a more specialized BLB1 system expressed mainly in the gut<sup>34</sup>. The present study reinforces the role of genetics in determining MHC type II gene composition, as BLB1 appears to be threefold more expressed in the pHu- jejunum and BLB2 twofold more expressed in the pHu+ jejunum.

Among the genes that participate in the immune response, DCLRE1C was also overexpressed in the pHu-line and located in one of the major regions under selection identified from the first to the fifth generation. DCLRE1C encodes the ARTEMIS protein, which plays a crucial role in V(D)J DNA recombination, a process that occurs in the early stages of B and T lymphocyte maturation and allows lymphocyte diversity<sup>35</sup>. All these results suggest that selection for an increased pHu, and therefore a reduction in muscle glycogen reserves, is associated with a degradation of the gut immune response in broilers. The roles of the expressional and positional candidate genes identified in this study and, more generally, the mechanisms linking gut health and muscle glycogen reserves remain to be elucidated.

One of the questions addressed by our study was to assess the extent of variations in muscle glycogen, which could be linked to possible modifications in the digestive microbiota. We focused on the caecal microbiota, which is the most abundant and representative of the digestive microbiota. The bacterial species richness was greater in the pHu lines than in the Ross 308 broilers at the same age of development<sup>36</sup>. Increased species diversity is known to give broilers the ability to slow pathogen colonization, an indicator of their good health<sup>37</sup> and has been shown to be lower in fast-growing broilers reared indoors than in slow-growing broilers reared outside<sup>36</sup>. Despite similar bacterial diversity, three bacterial genera, whose abundance represented less than 1% of the total microbiota, differed between the two divergent lines. The first genus, *Lachnospira*, which was more abundant in the pHu-line, is of particular interest because of its ability to metabolize lactate and acetate into butyrate and propionate, thus promoting mucin production<sup>38</sup>. Its second function concerns intestinal health, as it is able to metabolize fermentable carbohydrates, thus influencing glucose metabolism. The second genus, *Lachnospiraceae UCG-010*, which was also more abundant in the pHu-line, is able to degrade fructose and produce lactate<sup>39</sup>. It is also associated with intestinal homeostasis and immunity, and its presence is associated with improved intestinal immunity and increased mucus production<sup>40</sup>. The third genus, *Caproiciproducens*, which was overexpressed in the pHu+line, is able to produce caproic acid for use as an energy source<sup>41</sup>.

These subtle, albeit minute, variations have the potential to influence two important metabolic pathways in prokaryotes, which were more abundant in the pHu-line. The first pathway identified concerns carbon fixation in prokaryotes, a crucial energy process used by autotrophic bacteria. This process remains extremely complex due to the large number of possible metabolic pathways involved. Carbon fixation represents a vital step for autotrophic organisms, converting inorganic carbon (e.g., CO<sub>2</sub>) into organic compounds. Of the available pathways, only two are relevant. The reductive citric acid cycle (Arnon-Buchanan cycle), present in microaerophiles and anaerobes, involves the fixation of four CO<sub>2</sub> molecules to produce oxaloacetate<sup>42</sup>. Alternatively, the acetyl-CoA reduction pathway (Wood-Ljungdahl pathway), present in strictly anaerobic bacteria, some of which produce methane, uses a bifunctional enzyme to convert CO<sub>2</sub> to acetyl-CoA 3-hydroxypropionate-hydroxybutyrate<sup>43</sup>.

The second pathway is the citrate cycle, also known as the Krebs cycle, which is a fundamental metabolic pathway found in most living organisms, including bacteria. It plays an essential biochemical role, allowing the breakdown of various carbon molecules (carbohydrates, lipids, amino acids) to produce energy in the form of adenosine triphosphate (ATP) and other intermediates. In bacteria, the Krebs cycle occurs in the mitochondrial matrix, the intracellular space of bacteria. The citrate cycle is critical to bacterial metabolism, providing not only energy in the form of ATP but also essential precursors for other metabolic pathways, including the biosynthesis of amino acids and nucleotide bases<sup>44</sup>.

This study is the first to examine the role of intestinal function in the control of muscle glycogen stores in chickens. The results revealed several differences in digestive tract anatomy and apparent feed digestibility, suggesting greater nutrient availability in the pHu-chicken line, which has very high glycogen levels. Molecular analysis at the jejunal level also suggested the involvement of other local or more central processes, such as the immune response, tissue morphogenesis and the regulation of food intake, which could modulate the intake and/or metabolic utilization of nutrients. The next step will be to carry out a joint analysis of the transcriptional regulation observed at the intestinal and muscular levels to better assess the involvement of the phenotypic and molecular changes observed in the control of muscle glycogen reserves in chickens.

## Materials and methods

All animal care and experimental procedures required for this study were conducted in accordance with the French Animal Welfare Act and were approved by the Ethics Committee Val de Loire under the project reference APAFIS#30,842–2,021,040,107,513,853 v3. The Ethics Committee is registered with the National Committee under the number D371751. The ARRIVE guidelines have been followed in the reporting of this animal research.

## Experimental design

The chickens come from divergent pHu+ and pHu- lines selected by INRAE over 15 generations. A total of 80 chicks were hatched and reared at the PEAT INRAE Poultry Experimental Facility (INRAE, Centre Val de Loire, Nouzilly, France)<sup>45</sup>. The pHu+ and pHu- lines were selected on the basis of the ultimate pH of the *pectoralis major* breast muscle, resulting in significant differences in muscle glycogen content and meat quality<sup>8</sup>. Chickens from the two lines were reared together in the same room under classical conditions until 29 days of age. The chickens had ad libitum access to food and water. From Days 1 to 20, they received a conventional diet, and from Days 21 to 29, they received the same diet containing 0.4% of the nondigestible marker titanium dioxide (TiO<sub>2</sub>). On Day 28, all birds were weighed, and 15 chickens per line were selected on the basis of their pedigree to represent as many families as possible within a line and to be representative of their group in terms of body weight. On Day 29, blood samples were taken from the occipital sinus to recover plasma after centrifugation and stored at –80 °C. Then, they were euthanized using a lethal dose of dolethal to perform measurements and sampling of several tissues and digestive contents.

### Sample collection and anatomical characterization of the digestive tract

The proventriculus plus gizzard, duodenum, jejunum, ileum, and caeca were anatomically dissected, washed and weighed. One sample of the jejunum, including its three concentric layers—the mucosa, the muscularis and the serosa—was immediately preserved in ethanol. The content of the distal part of the ileum was sampled and weighed to measure the ileal digestibility levels of calcium, phosphorus and nitrogen, as was the content of the caeca for analysis of the microbiota. Samples of the jejunum and *pectoralis major* muscle were quickly frozen in liquid nitrogen and then stored at  $-80^{\circ}\text{C}$  for further phenotyping and molecular analyses.

### Determination of ileal calcium, phosphorus and nitrogen digestibility

The first step consisted of the acidic solubilization of feed and ileal digesta using a microwave before the calcium (Ca), phosphorus (P) and titanium (Ti) concentrations were determined via optical emission spectroscopy (ICAP 7000, Thermo Scientific). Nitrogen was measured in the diet and digesta of the distal part of the ileum (Kjeldahl method)<sup>46</sup>. The digestibility levels of calcium (Ca), phosphorus (P) and nitrogen (N) were then calculated according to the formula below on the basis of the measurement of the indigestible marker titanium (Ti):

$$\text{Ca, P and N digestibility (\%)} = 100 - \left(100 * \frac{\text{Ti Diet} * \text{Ca or P or N Digesta}}{\text{Ti Digesta} * \text{Ca or P or N Diet}}\right)$$

where Ti Diet and Ti Digesta = the concentration of titanium in the diet or digesta (g/kg); Ca or P or N Diet and Ca or P or N Digesta = the concentration of Ca or P or N analysed in the diet or in the digesta (g/kg).

### Histological and biochemical measurements

Paraffin-embedded 10  $\mu\text{m}$  serial sections were stained with haematoxylin–eosin (HE) and observed using a Nikon Eclipse 80i<sup>®</sup> microscope and NIS-Elements software. Structural histological measurements were performed blindly using a semiautomated macro with Fiji software (v.1.54f.)<sup>47</sup>. The following structural parameters were measured: total mucosal thickness, crypt depth, villus height, villus width, submucosal thickness and muscularis thickness. The villus/crypt ratio was also determined.

The levels of several metabolites were measured in the jejunum using commercial kits and according to the technical recommendations of the suppliers: alkaline phosphatase activity (N7660, N46451G, SIGMA), total antioxidant status (TAS, NX2332, RANDOX) and haptoglobin content (PHASE<sup>™</sup>, Haptoglobin Assay, Tridelata Development Ltd.).

Muscle glycolytic potential (GP) is an indicator of muscle glycogen content in living animals and is defined as the potential for lactic acid production during postmortem glycolysis. The protocol used to measure the glycolytic potential of the *pectoralis major* muscle was adapted from the method described by Monin and Sellier and was miniaturized to enable measurements to be taken from 100 mg of ground tissue under nitrogen<sup>48</sup>. The glycolytic potential was calculated using the following formula: potential glycolysis =  $2 * (\text{total glucose}) + (\text{lactate})$ , expressed as  $\mu\text{mol}$  lactate equivalent per gram of muscle.

### Statistical analyses of phenotypic traits

Statistical analyses were performed using RStudio software (v.4.3.3) (<http://www.rstudio.com/>)<sup>49</sup>. For anatomical, histological, digestibility and biochemical parameters, line effects were analysed by one-way ANOVA, considering a significance level of  $p \leq 0.05$ . Because all traits were normally distributed, means were compared using Student's t test.

### Preparation of the jejunum for RNA-seq analysis

A NucleoSpin RNA kit (Macherey–Nagel, Nucleospin RNA, ref: 740,955.50) was used to extract total RNA from 30 mg of ground jejunum tissue under nitrogen according to the manufacturer's protocol. RNA quality was first checked using a spectrophotometer (NanoDrop, ND-1000) and after separation on agarose gels on an Agilent RNA Nano Assay chip (Agilent RNA 6000 Nano Reagents, ref: 5067–1511, Agilent Technologies) using an Agilent Bioanalyzer 2100 (Agilent Technologies). The RNA integrity numbers (RINs) of all RNA samples were greater than 9.1. RNA samples were then sequenced for  $2 \times 150$  bp on the NovaSeq 6000-A00318 sequencer (GeT-PlaGe facility, Toulouse, France) and multiplexed according to the standard Illumina XP sequencing protocol.

### RNA sequencing and differential gene expression analysis

The Nextflow nf-core/rnaseq analysis pipeline (Nextflow v.21.10.6 nf-core/rnaseq revision 3.5) was used with the version 7b release 109 of the Gallus gallus genome reference (Gallus\_gallus.bGal1.mat.broiler.GRCg7b.dna.toplevel.fa) and gene structure (Gallus\_gallus.bGal1.mat.broiler.GRCg7b.109.gtf). The STAR<sup>50</sup> (v.2.6.1d) and Salmon<sup>51</sup> (v.1.5.3) tools were used to align and quantify genes and transcripts, respectively, using the default configurations for each tool. Differential analysis was performed on CPM (counts-per-million) data with a generalized linear model using the DESeq2<sup>52</sup> (v.1.7.3) package within the Galaxy Migale interface<sup>53</sup>. For each gene, the size effect of the line was estimated by the model as  $\log_2\text{FoldChange}$  and the fold change of expression calculated as  $2^{\log_2(\text{FC})}$ . Genes were considered differentially abundant between the two lines when the p values adjusted by controlling the false-positive rate with Benjamini–Hochberg correction were less than 0.05.



### Functional annotation and enrichment analysis of DE genes using ViSEAGO

Gene Ontology analysis was performed using the Visualization, Semantic similarity, and Enrichment Analysis of Gene Ontology (ViSEAGO)<sup>54</sup> package (v.1.12.0). GO annotations were retrieved from EntrezGene for the *Gallus gallus* species (ID = “9031”) using ViSEAGO EntrezGene2GO followed by functional annotation. ViSEAGO uses topGO to perform GO term enrichment tests on the sets of genes of interest (DE genes). We used the biological process ontology category with Fisher’s exact test (classic algorithm), and a p value less than 0.01 was considered to indicate statistical significance. The results of the enrichment tests were then hierarchically grouped based on Wang’s semantic similarity distance and the ward.D2 aggregation criterion. The results were visualized on a heatmap where GO terms are ordered by hierarchical clustering based on their functional similarity, and GO term enrichment significance is shown as a colour gradient ( $-\log_{10}$  p value).

### Colocalization between DE genes and QTLs or selection signatures identified in the pHu lines

The physical positions of the genes differentially expressed in the jejunum were compared with genomic regions of interest (QTLs for breast or thigh meat ultimate pH and selection signatures) previously identified in the two divergent lines using the GalGal5 assembly<sup>18</sup>. To this end, QTLs and selection signatures were repositioned on the GalGal7 reference genome by mapping the SNPs (=QTLs) over a distance of  $\pm 150$  bp and the regions over  $\pm 250$  bp. SAMtools (v.1.16.1) was used to extract subsequences from the GalGal7-indexed reference sequence, after which the chromosomes were renamed using the Ensembl nomenclature. Subsequently, we aligned the subsequences extracted from the GalGal5 genome to those of GalGal7 using BWA (v.0.7.17), a commonly used tool for aligning genomic sequences. These steps enabled us to update the positions of the majority of the QTLs and regions of interest in the GalGal7 reference genome.

### Determination of bacterial diversity in the caecal microbiota by 16S rRNA sequencing

RNA was extracted from the caecal content using the QIAamp® DNA Mini Kit (ref: 51,304, QIAGEN) according to the supplier’s recommendations. After extraction, the quality of the bacterial RNA extracts was checked using a NanoDrop (ND-1000). Targeted amplification was then performed, concentrating on the V3 and V4 variable regions of the 16S rRNA. These regions are known to be informative for microbiota identification. The V3-V4 regions were amplified from purified genomic DNA through a 30-cycle amplification process performed at an annealing temperature of 65 °C using the forward primer F343 (CTTTCCCTACACGACGCTCTTCCGATCTTACGGRAGGCAGCAG) and the reverse primer R784 (GGA GTTCAGACGTGTGCTCTTCCGATCTTACCAGGGTATCTAATCCT). One single multiplex was performed using a homemade 6 bp index, which was added to R784 during a second 12-cycle amplification process using a forward primer (AATGATACGCGACCACCGAGATCTACACTCTTTCCCTACACGAC) and a corresponding reverse primer (CAAGCAGAAGACGGCATAACGAGAT-index-GTGACTGGAGTTCAGACGT GT). The resulting PCR products were purified and loaded onto an Illumina MiSeq cartridge according to the manufacturer’s instructions. The quality of the run was checked internally using PhiX, and then each paired-end sequence was assigned to its sample with the help of the previously integrated index.

The bioinformatic processing of sequence reads obtained was performed using the FROGS (Find Rapidly OTUs with Galaxy Solution) pipeline (v.4.0.1) within the Galaxy Migale interface<sup>53</sup>. A preprocessing tool was used to remove sequences not related to the two primers, to trim the primers and to remove all sequences containing ambiguous bases. Sequence clustering was performed with the Swarm<sup>55</sup> algorithm (v.3.0.0). Chimeric sequences were detected with the VSEARCH<sup>56</sup> algorithm (v.2.17.0) and removed. A filtering tool was used to remove false clusters with a prevalence less than or equal to 3 and a minimum of read abundances less than 5e-05 of the total number of reads. The filtered sequences were assigned to taxa with BLAST affiliations<sup>55,56</sup> (v.2.10) and the 16S\_SILVA\_138.1 database.

Sequences were clustered into OTUs with similarity and coverage thresholds of 90% for analysis using Easy16S (<https://shiny.migale.inrae.fr/app/easy16S>).

The biostatistical processing of sequences was performed using the FROGSFUNC pipeline, which consists of 4 main steps. The OTUs were first positioned in a reference phylogenetic tree, then their abundances and functions were calculated for each sample. Finally, metabolic pathway abundance was calculated for each sample using the KEGG database<sup>55,56</sup>.

### Data availability

The RNA-seq and 16S raw data sets generated and analyzed during the current study are available through the link: <https://dataview.ncbi.nlm.nih.gov/object/PRJNA1120343?reviewer=hvs7vbe4hlp0brauitlevmm0p>.

Received: 14 June 2024; Accepted: 23 September 2024

Published online: 15 October 2024

### References

1. OECD Agriculture Statistics. <https://doi.org/10.1787/agr-data-en> (OECD Publishing).
2. Barbut, S. Problem of pale soft exudative meat in broiler chickens. *Br. Poult. Sci.* **38**, 355–358 (1997).
3. Zhang, L. & Barbut, S. Rheological characteristics of fresh and frozen PSE, normal and DFD chicken breast meat. *Br. Poult. Sci.* **46**, 687–693 (2005).
4. Petracci, M., Bianchi, M. & Cavani, C. The European perspective on pale, soft, exudative conditions in poultry. *Poult. Sci.* **88**, 1518–1523 (2009).
5. Petracci, M. & Cavani, C. Muscle growth and poultry meat quality issues. *Nutrients* **4**, 1–12 (2011).
6. Le Bihan-Duval E. et Berri C. Poultry Quality Evaluation. Woodhead Publishing Elsevier. in p 199.
7. Le Bihan-Duval, E. et al. Chicken meat quality: genetic variability and relationship with growth and muscle characteristics. *BMC Genet.* **9**, 53 (2008).

8. Alnahhas, N. et al. Selecting broiler chickens for ultimate pH of breast muscle: Analysis of divergent selection experiment and phenotypic consequences on meat quality, growth, and body composition traits. *J. Anim. Sci.* **92**, 3816–3824 (2014).
9. Alnahhas, N. et al. Impact of divergent selection for ultimate pH of pectoralis major muscle on biochemical, histological, and sensorial attributes of broiler meat. *J. Anim. Sci.* **93**, 4524–4531 (2015).
10. Alnahhas, N. et al. Genetic parameters of white striping in relation to body weight, carcass composition, and meat quality traits in two broiler lines divergently selected for the ultimate pH of the pectoralis major muscle. *BMC Genet.* **17**, 61 (2016).
11. Métayer-Coustard, S. et al. Early growth and protein-energy metabolism in chicken lines divergently selected on ultimate pH. *Front. Physiol.* **12**, 643580 (2021).
12. Le Bihan-Duval, E. et al. Genetic variability of chick quality within two chicken lines differing for glycogen reserves (2022).
13. Erensoy, K. et al. Research note: Divergent selection for breast muscle ultimate pH affects egg quality traits in broiler breeders. *Poult. Sci.* **101**, 102142 (2022).
14. Petit, A. et al. Nutrient sources differ in the fertilised eggs of two divergent broiler lines selected for meat ultimate pH. *Sci. Rep.* **12**, 5533 (2022).
15. Beaucercq, S. et al. Serum and muscle metabolomics for the prediction of ultimate pH, a key factor for chicken-meat quality. *J. Proteome Res.* **15**, 1168–1178 (2016).
16. Beaucercq, S. et al. Muscle transcriptome analysis reveals molecular pathways and biomarkers involved in extreme ultimate pH and meat defect occurrence in chicken. *Sci. Rep.* **7**, 6447 (2017).
17. Berger, Q. et al. Profiles of genetic parameters of body weight and feed efficiency in two divergent broiler lines for meat ultimate pH. *BMC Genomic Data* **23**, 18 (2022).
18. Bihan-Duval, E. L. et al. Identification of genomic regions and candidate genes for chicken meat ultimate pH by combined detection of selection signatures and QTL. *BMC Genomics* **19**, 294 (2018).
19. Nay, K. et al. Gut bacteria are critical for optimal muscle function: a potential link with glucose homeostasis. *Am. J. Physiol.-Endocrinol. Metab.* **317**, E158–E171 (2019).
20. Mignon-Grasteau, S. et al. Impact of selection for digestive efficiency on microbiota composition in the chicken. *PLOS ONE* **10**, e0135488 (2015).
21. Lv, H. et al. Microbial composition in the duodenum and ileum of yellow broilers with high and low feed efficiency. *Front. Microbiol.* **12**, 689653 (2021).
22. Dittoe, D. K., Olson, E. G. & Ricke, S. C. Impact of the gastrointestinal microbiome and fermentation metabolites on broiler performance. *Poult. Sci.* **101**, 101786 (2022).
23. Zhao, Y. & Zou, D. W. Gut microbiota and irritable bowel syndrome. *J. Dig. Dis.* <https://doi.org/10.1111/1751-2980.13204> (2023).
24. De Verdal, H. et al. Digestive tract measurements and histological adaptation in broiler lines divergently selected for digestive efficiency. *Poult. Sci.* **89**, 1955–1961 (2010).
25. Svihus, B. Function of the digestive system. *J. Appl. Poult. Res.* **23**, 306–314 (2014).
26. Hurwitz, S., Bar, A. & Cohen, I. Regulation of calcium absorption by fowl intestine. *Am. J. Physiol.-Leg Content* **225**, 150–154 (1973).
27. Rideau, N. et al. The gastric isthmus from D+ and D- broiler lines divergently selected for digestion efficiency shows histological and morphological differences. *Poult. Sci.* **93**, 1245–1250 (2014).
28. Williams, G. et al. The hypothalamus and the control of energy homeostasis. *Physiol. Behav.* **74**, 683–701 (2001).
29. Murugesan, S. & Nidamanuri, A. L. Role of leptin and ghrelin in regulation of physiological functions of chicken. *Worlds Poult. Sci. J.* **78**, 1021–1036 (2022).
30. Peeters, T. L. Ghrelin: a new player in the control of gastrointestinal functions. *Gut* **54**, 1638–1649 (2005).
31. Wang, Z., Yang, W. L., Jacob, A., Aziz, M. & Wang, P. Human ghrelin mitigates intestinal injury and mortality after whole body irradiation in rats. *PLOS ONE* **10**, e0118213 (2015).
32. Rogers, S. L. et al. Characterization of the chicken C-Type lectin-like receptors B-NK and B-lec suggests that the NK complex and the MHC share a common ancestral region. *J. Immunol.* **174**, 3475–3483 (2005).
33. Strand, T., Wang, B., Meyer-Lucht, Y. & Höglund, J. Evolutionary history of black grouse major histocompatibility complex class IIB genes revealed through single locus sequence-based genotyping. *BMC Genet.* **14**, 29 (2013).
34. Parker, A. & Kaufman, J. What chickens might tell us about the MHC class II system. *Curr. Opin. Immunol.* **46**, 23–29 (2017).
35. Rohr, J. et al. Chronic inflammatory bowel disease as key manifestation of atypical ARTEMIS deficiency. *J. Clin. Immunol.* **30**, 314–320 (2010).
36. Ocejo, M., Oporto, B. & Hurtado, A. 16S rRNA amplicon sequencing characterization of caecal microbiome composition of broilers and free-range slow-growing chickens throughout their productive lifespan. *Sci. Rep.* **9**, 2506 (2019).
37. Di Marcantonio, L. et al. Investigating the cecal microbiota in broiler poultry farms and its potential relationships with animal welfare. *Res. Vet. Sci.* **144**, 115–125 (2022).
38. Dimidi, E., Christodoulides, S., Scott, S. M. & Whelan, K. Mechanisms of action of probiotics and the gastrointestinal microbiota on gut motility and constipation. *Adv. Nutr.* **8**, 484–494 (2017).
39. Atzeni, A. et al. Taxonomic and functional fecal microbiota signatures associated with insulin resistance in non-diabetic subjects with overweight/obesity within the frame of the PREDIMED-plus study. *Front. Endocrinol.* **13**, 804455 (2022).
40. Yang, B. et al. Lactobacillus ruminis alleviates DSS-induced colitis by inflammatory cytokines and gut microbiota modulation. *Foods* **10**, 1349 (2021).
41. Kim, B.-C. et al. Caproiciproducens galactitolivorans gen. nov., sp. nov., a bacterium capable of producing caproic acid from galactitol, isolated from a wastewater treatment plant. *Int. J. Syst. Evol. Microbiol.* **65**, 4902–4908 (2015).
42. Ljungdhal, L. G. The autotrophic pathway of acetate synthesis in acetogenic bacteria. *Annu. Rev. Microbiol.* **40**, 415–450 (1986).
43. Zarzycki, J., Brecht, V., Müller, M. & Fuchs, G. Identifying the missing steps of the autotrophic 3-hydroxypropionate CO<sub>2</sub> fixation cycle in *Chloroflexus aurantiacus*. *Proc. Natl. Acad. Sci.* **106**, 21317–21322 (2009).
44. De Vos, W. M., Tilg, H., Van Hul, M. & Cani, P. D. Gut microbiome and health: mechanistic insights. *Gut* **71**, 1020–1032 (2022).
45. PEAT. Poultry Experimental Facility. (2018) <https://doi.org/10.15454/1.5572326250887292E12>.
46. Kjeldahl, J. Neue Methode zur Bestimmung des Stickstoffs in organischen Körpern. *Fresenius Z. Für Anal. Chem.* **22**, 366–382 (1883).
47. Schindelin, J. et al. Fiji: an open-source platform for biological-image analysis. *Nat. Methods* **9**, 676–682 (2012).
48. Monin, G. & Sellier, P. Pork of low technological quality with a normal rate of muscle pH fall in the immediate post-mortem period: The case of the Hampshire breed. *Meat Sci.* **13**, 49–63 (1985).
49. Allaire, J. RStudio: integrated development environment for R. *Boston MA* **770**, 165–171 (2012).
50. Dobin, A. et al. STAR: ultrafast universal RNA-seq aligner. *Bioinformatics* **29**, 15–21 (2013).
51. Patro, R., Duggal, G., Love, M. I., Irizarry, R. A. & Kingsford, C. Salmon provides accurate, fast, and bias-aware transcript expression estimates using dual-phase inference. *BioRxiv* **1**, 9 (2015).
52. Varet, H., Brillet-Guéguen, L., Coppée, J.-Y. & Dillies, M.-A. SARTools: A DESeq2- and EdgeR-Based R Pipeline for Comprehensive Differential Analysis of RNA-Seq Data. *PLOS ONE* **11**, e0157022 (2016).
53. MIGALE. Migale Bioinformatics Facility. (2018) <https://doi.org/10.15454/1.5572390655343293E12>.
54. Brionne, A., Juanchich, A. & Hennequet-Antier, C. ViSEAGO: a Bioconductor package for clustering biological functions using Gene Ontology and semantic similarity. *BioData Min.* **12**, 16 (2019).
55. Escudié, F. et al. FROGS: find, rapidly, OTUs with galaxy solution. *Bioinformatics* **34**, 1287–1294 (2018).

56. Bernard, M., Rué, O., Mariadassou, M. & Pascal, G. FROGS: a powerful tool to analyse the diversity of fungi with special management of internal transcribed spacers. *Brief. Bioinform.* **22**, bbab318 (2021).

## Acknowledgements

The authors thank numerous unnamed members of the experimental unit PEAT and research unit BOA for their technical assistance in animal rearing and laboratory analyses, respectively. We also wish to thank Christelle Hennequet-Antier, Amélie Juanchich and Aurélien Brionne (from INRAE) for their advice regarding RNA sequencing analyses, and the Genotoul Bioinformatics platform Toulouse Occitanie (Bioinfo Genotoul, <https://doi.org/10.15454/1.5572369328961167E12>) for providing help, computing and storage resources. All our work and results are based on the Genotoul Bioinformatics hardware infrastructure and the GeT-PLaGe platform for the 16S sequencing.

## Author contributions

E.L.B.D. and C.B. designed the experiments and supervised the study. P.B. performed the experiments and laboratory analyses under the supervision of E.L.B.D., C.B., S.M.C. and A.N. P.B. performed all statistical and functional analyses of RNA and 16S sequencing. S.M.H. performed the bioinformatic analyses of the RNA-Seq. J.P. and C.R. performed the histological analyses. P.B. drafted the first version of the manuscript under the supervision of E.L.B.D. and C.B. All authors read, enriched and approved the final manuscript. All authors approved the final version of the manuscript.

## Funding

This work was supported by INRAE.

## Competing interests

The authors declare no competing interests.

## Additional information

**Supplementary Information** The online version contains supplementary material available at <https://doi.org/10.1038/s41598-024-74009-z>.

**Correspondence** and requests for materials should be addressed to C.B. or E.L.-D.

**Reprints and permissions information** is available at [www.nature.com/reprints](http://www.nature.com/reprints).

**Publisher's note** Springer Nature remains neutral with regard to jurisdictional claims in published maps and institutional affiliations.

**Open Access** This article is licensed under a Creative Commons Attribution-NonCommercial-NoDerivatives 4.0 International License, which permits any non-commercial use, sharing, distribution and reproduction in any medium or format, as long as you give appropriate credit to the original author(s) and the source, provide a link to the Creative Commons licence, and indicate if you modified the licensed material. You do not have permission under this licence to share adapted material derived from this article or parts of it. The images or other third party material in this article are included in the article's Creative Commons licence, unless indicated otherwise in a credit line to the material. If material is not included in the article's Creative Commons licence and your intended use is not permitted by statutory regulation or exceeds the permitted use, you will need to obtain permission directly from the copyright holder. To view a copy of this licence, visit <http://creativecommons.org/licenses/by-nc-nd/4.0/>.

© The Author(s) 2024